

# Photorefractive planar waveguides in BaTiO<sub>3</sub> fabricated by ion-beam implantation

K. E. Youden, S. W. James, and R. W. Eason

*Department of Physics and Optoelectronics Research Centre, University of Southampton, Southampton SO9 5NH, UK*

P. J. Chandler, L. Zhang, and P. D. Townsend

*School of Mathematical and Physical Sciences, University of Sussex, Brighton BN1 9QH, UK*

Received June 16, 1992

For the first time to our knowledge, photorefractive properties have been observed in planar waveguides fabricated by the technique of ion-beam implantation in BaTiO<sub>3</sub> single crystals. The implantation was carried out by using 1.5-MeV H<sup>+</sup> ions at a dose of 10<sup>-16</sup> ions/cm<sup>2</sup>. For a given input power, a decrease in the effective photorefractive two-beam coupling response time of  $\geq 10^2$  has been observed, owing to a combination of optical confinement within the waveguide and possible modification of charge-transport properties induced through implantation. Experiments carried out on the two-beam coupling gain show that the gain direction has been reversed in the waveguide compared with that of the bulk crystal.

Photorefractive nonlinear optical crystals, such as BaTiO<sub>3</sub> and Sr<sub>x</sub>Ba<sub>1-x</sub>Nb<sub>2</sub>O<sub>6</sub> (SBN), are currently used for a wide range of applications in optical phase conjugation and two- and four-wave mixing techniques.<sup>1</sup> The fabrication of photorefractive waveguides is desirable because it provides compatibility with other miniaturized integrated-optical waveguide devices in common use today, in particular with laser diodes and fiber geometries. Additionally, the optical confinement inherent to waveguide structures allows a high intensity to be maintained within the crystalline waveguide, and this increased intensity-length product leads to an appreciable decrease in the effective photorefractive response time for a given input power. BaTiO<sub>3</sub> is perhaps the most interesting material for nonlinear optical applications, because of the very large value of its electro-optic coefficient,  $r_{42} = r_{51} = 1640$  pm/V,<sup>2</sup> which is one of the largest values known for any material.

Thin films and waveguides of BaTiO<sub>3</sub> have previously been fabricated by several techniques, including He<sup>+</sup> implantation,<sup>3</sup> molecular beam epitaxy,<sup>4</sup> pulsed laser deposition,<sup>5</sup> and the sol-gel process,<sup>6</sup> but in all these reports the important photorefractive properties were either not retained or not reported. Additionally, slab waveguides (70–100 μm) have also been prepared in BaTiO<sub>3</sub>,<sup>7</sup> in which photorefractive intermode coupling effects have been observed. In order to produce such a photorefractive waveguide, there are several criteria that need to be satisfied. First, to obtain a waveguide, a low-loss, light-confining region must be created. Second, for a waveguide in BaTiO<sub>3</sub> to be photorefractive it must be of the correct crystalline phase, poled, and electro-optic and the photorefractive donor/acceptor mechanism must be retained. The importance of satisfying all these criteria simultaneously has been

highlighted in recent research carried out at our laboratory on He<sup>+</sup> ion-implanted waveguides in SBN and Bi<sub>12</sub>SiO<sub>20</sub>. In the case of Bi<sub>12</sub>SiO<sub>20</sub> the intensity-dependent photochromic properties<sup>8</sup> produced such high losses in the waveguide as to make characterization complicated. For SBN, the waveguide losses were high ( $\approx 25$  dB cm<sup>-1</sup>), but this did not preclude experiments to determine that the waveguide was still electro-optic. No photorefractive properties were observed for the SBN waveguide, however, despite the bulk crystal's being photorefractive. This is believed to be due to disruption of the photorefractive mechanism caused by the He<sup>+</sup> implantation process at the doses used so far. In the case of BaTiO<sub>3</sub> additional processing problems exist because of the phase transitions from tetragonal to orthorhombic and tetragonal to cubic, which occur at  $\approx 9^\circ\text{C}$  and  $\approx 130^\circ\text{C}$ , respectively.<sup>2</sup>

In this Letter we describe what is to our knowledge the first achievement of a photorefractive planar waveguide in BaTiO<sub>3</sub>, produced by high-energy H<sup>+</sup> ion implantation. 1.5-MeV H<sup>+</sup> ions at a dose of 10<sup>16</sup> ions/cm<sup>2</sup> were implanted into a flat polished face of a single crystal, which was held at room temperature during implantation. The implanting ion-beam direction was nominally perpendicular to the plane containing the crystal *c* axis. On entering the crystal, the ions initially lose energy through electronic excitations with the lattice atoms, but this is not generally responsible for causing displacement damage. However, the ionizing effect of the implanted ion can produce undesirable color-center defects that may be responsible for increased propagation loss. Once they have a sufficiently low energy, the ions undergo nuclear collisions that displace lattice atoms and distort the crystal lattice, which leads to the creation of a sharply defined layer of lower refractive

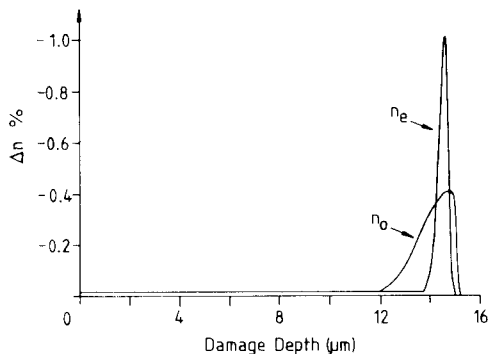


Fig. 1. Inferred refractive-index profiles for the ordinary and extraordinary rays at  $\lambda = 633$  nm.

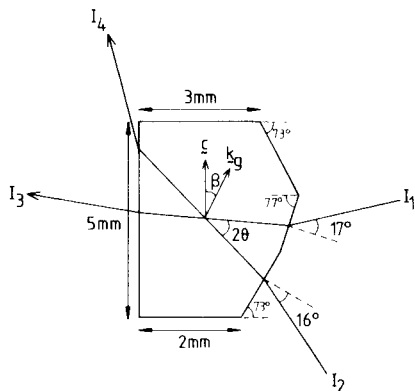


Fig. 2. Details of the crystal dimensions and angles of precise polished faces ( $\mathbf{k}_g$  is the grating wave vector).

index.<sup>9</sup> If correctly launched, light can then be confined between the polished top surface of the crystal and this low-index damage barrier.

Both TE and TM waveguide modes were investigated by using the dark mode<sup>10</sup> characteristics observed by prism coupling. From these data, the ordinary and extraordinary refractive-index profiles  $n_o$  and  $n_e$  were inferred,<sup>11</sup> which are shown in Fig. 1. These inferred profiles indicate a waveguide depth of  $\approx 15$   $\mu\text{m}$  and with a simple analysis<sup>12</sup> predicted a waveguide capable of supporting  $\approx 20$  guided modes, which was verified experimentally. Waveguide losses were determined by end launching light into the waveguide at normal incidence to the crystal. A He-Ne laser at  $\lambda = 633$  nm was expanded to a beam diameter of  $\approx 4$  mm and then focused into the waveguide using  $4\times$  objectives. The output was collected by using a  $4\times$  objective and measured by using a calibrated power meter. Correcting for Fresnel reflections and assuming a launch efficiency of 80%, we measured a waveguide loss of  $\approx 14$  dB/cm. In other published research<sup>13</sup> the ion-implanted waveguide loss has been significantly reduced by annealing at approximately  $200^\circ\text{C}$  to remove any color-center defects created in the electronic stopping region as mentioned above. However, the Curie temperature of  $\approx 130^\circ\text{C}$  for  $\text{BaTiO}_3$  discouraged us from annealing, but as is described below, successful two-beam coupling was demonstrated despite the high waveguide loss because only a few millimeters of crystal is required to perform the two-beam coupling.

To characterize and quantify the photorefractive

properties of the waveguide a standard two-beam coupling arrangement was used. Three wavelengths (633, 568, and 488 nm) were used to perform the experiments, with extraordinary-polarized light used to access TE waveguide modes and hence the large  $r_{42}$  electro-optic coefficient of the crystal. For all wavelengths, the input laser beam was expanded to a diameter of  $\approx 4$  mm, and the total input power was varied by using a neutral-density wheel while keeping a beam intensity ratio ( $I_1/I_2$ ) of 1:3. By using  $4\times$  microscope objectives to focus the light to a beam waist of  $\approx 4$   $\mu\text{m}$ , two mutually coherent beams  $I_1$  and  $I_2$  were launched into the waveguide at the angles shown in Fig. 2. The input crystal faces had previously been cut and polished to facilitate end launching for two-beam coupling experiments, given the restrictive conditions imposed by the microscope objective launch. Outputs from the waveguide,  $I_3$  and  $I_4$ , were selectively imaged (again using a  $4\times$  microscope objective) onto a calibrated power meter.

From the beam-coupling measurements, it was observed that the direction of the two-beam coupling gain has been reversed in the waveguide compared with that in the bulk crystal. This provided additional confirmation that the photorefractive beam-coupling effects were indeed those present in the waveguide and were not just due to scattered light from the bulk or inadvertent bulk crystal coupling. The cause of the change in the gain direction is currently uncertain, but is likely to be due to a change in the dominant charge-carrier species<sup>14</sup> (from holes to electrons) brought about by the implantation process. Further research is currently being carried out to confirm this hypothesis.

The photorefractive response time  $\tau$ , as defined in Fig. 3, was measured for various total incident beam powers in both the waveguide and the bulk crystal. Figure 4 shows the measured response time ( $\tau$ ) versus the total input power at 488 nm. It can be seen that a considerable effective speedup has been achieved as anticipated. At the moderate input power of 70 mW a response time of 280  $\mu\text{s}$  was obtained in the waveguide, whereas the corresponding response time at the same input power in the bulk crystal was only 52 ms, a factor of  $\geq 10^2$  slower. In Fig. 4 the gradients for the response time versus the incident power ( $\tau \propto I^{-x}$ ) for the bulk and waveguide data were  $x \approx 0.6$  and 0.8, respectively. This difference is probably due to the proposed change in the

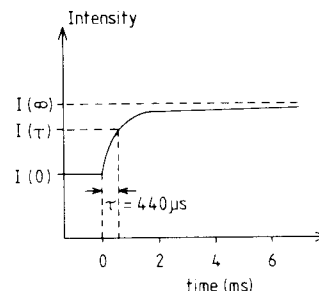


Fig. 3. Experimental rise time profile for the waveguide indicating the definition of the response time,  $I(\tau) = (1 - e^{-1})[I(\infty) - I(0)]$ . The figure is a trace from a digitizing oscilloscope output.

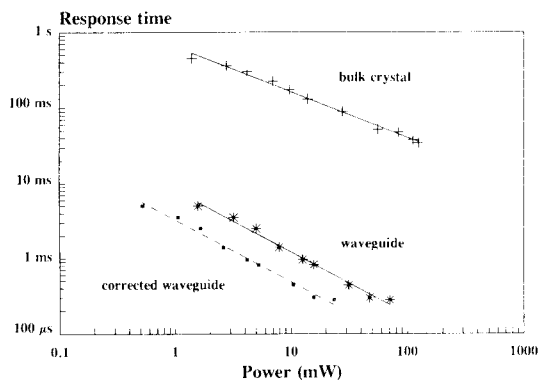


Fig. 4. Two-beam coupling response time versus the incident power for waveguide (\*) and bulk (+) crystal regions at  $\lambda = 488$  nm; the dashed line indicates the waveguide data corrected for measured waveguide losses of  $14 \text{ dB cm}^{-1}$ . For conversion to equivalent average irradiance, the beam area for bulk and waveguide measurements was estimated to be  $\approx 1 \times 10^{-2}$  and  $\approx 8 \times 10^{-6} \text{ cm}^2$ , respectively. The maximum irradiance obtained in the waveguide experiments therefore, with correction for inferred losses, was  $\approx 1.4 \text{ kW cm}^{-2}$ .

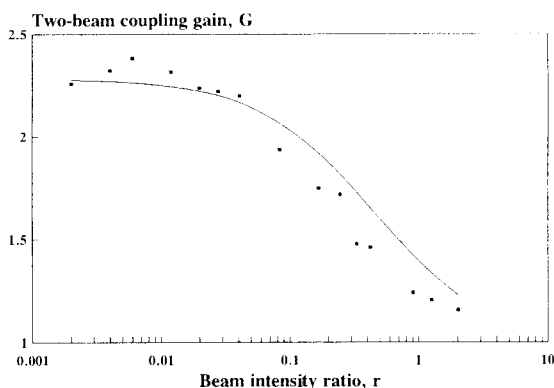


Fig. 5. Two-beam coupling gain  $G$  as a function of the beam intensity ratio  $r$  in the waveguide region at  $\lambda = 568$  nm. The solid curve represents the calculated profile from standard two-beam coupling theory.

dominant charge-carrier species and hence mobility. A further possibility for this difference in gradient is intensity-dependent absorption effects,<sup>15</sup> which can also modify gain and response time data. At present we are unable to expand on these effects, and further discussion awaits more systematic waveguide fabrication and characterization.

The same experimental arrangement was used to measure the effective two-beam coupling gain ( $G$ ) within the waveguide, defined as

$$G = \frac{I_3 \text{ with } I_2 \text{ present}}{I_3 \text{ without } I_2 \text{ present}}. \quad (1)$$

As stated above, the effective gain direction has been reversed in the guide compared with that in the bulk crystal so that for two-beam coupling in the guide,  $I_3$  experiences gain, whereas for the bulk,  $I_4$  shows gain. Values of  $G$  were measured at a wavelength of 568 nm as a function of the incident beam ratio,  $r = I_1/I_2$ , and the experimental results are shown in Fig. 5. The interaction length ( $l$ ) was estimated to be  $\leq 0.5$  mm from calculations of the area and geometry of the beams in the waveguide. The ex-

pression  $G = \exp \Gamma l$  was used to calculate a value for the two-beam coupling gain coefficient ( $\Gamma$ ) for  $r \ll l$ . Taking data from the saturation region of Fig. 5, and with fixed angles of  $\theta = 7^\circ$  and  $\beta = 17^\circ$  (as shown in Fig. 2), we obtained  $\Gamma = 16.5 \text{ cm}^{-1}$ .

Self-pumped and mutually pumped phase conjugation have also been observed, which further enhances the potential for these waveguide structures and applications. Additionally, self-pumping characterization will permit the further optimization of the fabrication process.

In conclusion, we have fabricated for the first time to our knowledge photorefractive waveguides in  $\text{BaTiO}_3$  by the technique of ion-beam implantation. The expected decrease in the photorefractive response time as a result of the optical confinement in the waveguide has been observed, along with an unexpected change in the coupling direction. In future experiments we aim to improve the two-beam coupling response time and gain by reducing the crystal size (and therefore minimize transmission loss) to match the two-beam interaction length.

The authors gratefully thank D. Z. Anderson for the generous loan of the  $\text{BaTiO}_3$  crystal that was implanted and for much help and useful discussion and S. J. Field for assistance in precision edge polishing of the crystal. The authors also acknowledge the support of the Science and Engineering Research Council under grants GR/F-84256 and GR/H21531 and support for K. E. Youden in the form of a research studentship.

## References

1. P. Günter and J.-P. Huignard, *Photorefractive Materials and Their Applications II* (Springer-Verlag, Berlin, 1988).
2. A. R. Johnston and J. M. Weingart, *J. Opt. Soc. Am.* **55**, 828 (1965).
3. P. Moretti, P. Thevenard, G. Godefroy, R. Sommerfeldt, P. Hertel, and E. Kräzig, *Phys. Status Solidi A* **117**, K85 (1990).
4. R. A. McKee, F. J. Walker, J. R. Conner, E. D. Specht, and D. E. Zelmon, *Appl. Phys. Lett.* **59**, 782 (1991).
5. K. Nashimoto, D. K. Fork, and T. H. Geballe, *Appl. Phys. Lett.* **60**, 1199 (1992).
6. M. N. Kamalasanan, S. Chandra, P. C. Joshi, and A. Mansingh, *Appl. Phys. Lett.* **59**, 3547 (1991).
7. B. Fischer and M. Segev, *Appl. Phys. Lett.* **54**, 684 (1989).
8. N. A. Vainos, S. L. Clapham, and R. W. Eason, *Appl. Opt.* **28**, 4381 (1989).
9. P. D. Townsend, *Nucl. Instrum. Phys. Res. B* **46**, 18 (1990).
10. P. K. Tein, R. Ulrich, and R. J. Martin, *Appl. Phys. Lett.* **14**, 291 (1969).
11. P. J. Chandler and F. L. Lama, *Opt. Acta* **33**, 127 (1986).
12. H. Kogelnik and V. Ramaswamy, *Appl. Opt.* **13**, 1857 (1974).
13. J. Y. C. Wong, L. Zhang, G. Kakarantzas, P. D. Townsend, P. J. Chandler, and L. A. Boatner, *J. Appl. Phys.* **71**, 149 (1992).
14. S. Ducharme and J. Feinberg, *J. Opt. Soc. Am. B* **3**, 283 (1986).
15. G. A. Brost, R. A. Motes, and J. R. Rotge, *J. Opt. Soc. Am. B* **5**, 1879 (1988).